Electronic Supplementary Material (ESI) for Catalysis Science & Technology.
This journal is © The Royal Society of Chemistry 2020

SUPPLEMENTARY MATERIAL

NANOSTRUCTURED IRON OXIDES STABILIZED BY CHITOSAN: USING COPPER TO ENHANCE DEGRADATION BY A COMBINED MECHANISM

Aline Aparecida Caetano[a], Pricila Maria Batista Chagas[a], Sara Silveira Vieira[b], Thais Fernandes Moratta[a], Júlio César De Souza Terra[c], José Domingos Ardisson[d], Iara do Rosário Guimarães[a*]

[a]Laboratório de Catálise Ambiental e Novos Materiais, Departamento de Química, Universidade Federal de Lavras, CEP 37200-000, Lavras, MG, Brazil.

[b] Laboratório de Química, Departamento de Química, Universidade Federal de Minas Gerais, CEP 31270-901, Belo Horizonte, MG, Brazil.

[c]Center for Green Chemistry and Catalysis, Departamento f Chemistry, McGill University, 801 Sherbrooke St. West, Montreal, QC, H3A-0B8, Canada.

[d]Laboratório de Física Aplicada, Centro de Desenvolvimento da Tecnologia Nuclear, CEP 30123-970, Belo Horizonte, MG, Brazil.

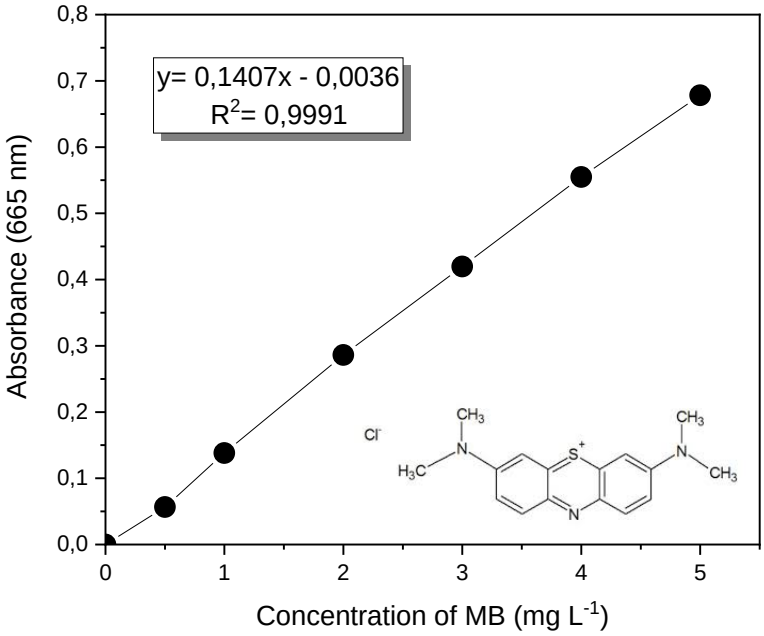

Fig. S1 Calibration curve of methylene blue (MB). MB structure (inset).

Table S1 Quantitative data for optimization of hydrogen peroxide (H_2O_2) concentration in the reaction medium.

Amount of H_2O_2 35% (µL)	**[H_2O_2] (mmol L^{-1})**
15	6,130
30	12,26
75	30,65
150	61,30
225	91,95
300	122,6

Table S2 Assignation of FTIR absorption bands of chitosan.

Wavenumber (cm^{-1})	Assignments	References
3353	N-H stretching	1, 2
3287	O-H stretching	
2924 and 2870	C-H symmetric and asymmetric stretching, respectively	
1645	C=O stretching of amide I	2-4
1591	N-H stretching of primary amine	2
1416 and 1374	CH_2 and CH_3 symmetric deformation, respectively	
1317	C-N stretching of amide III	1,5
1262	O-H bending vibrations of chitosan	2
1151	asymmetric stretching of the C-O-C bridge	3
1062 and 1025	C-O stretching	4,5
897	C-H bending out of the plane of the ring of monosaccharides	1,2

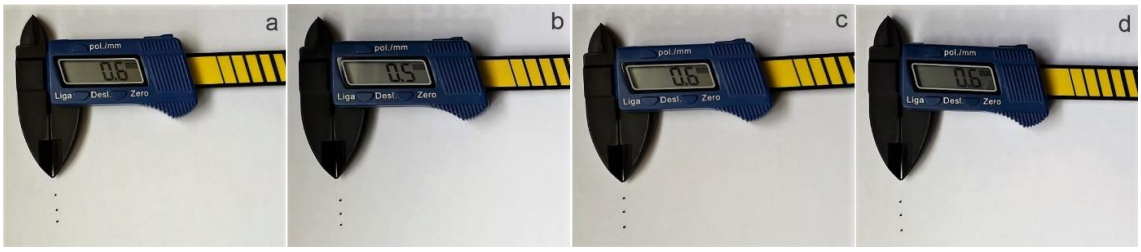

Fig. S2 Average size of beads selected by digital caliper (Eccofer®) a) CSFe b) $CSFeCu_5$ c) $CSFeCu_{10}$ d) $CSFeCu_{15}$.

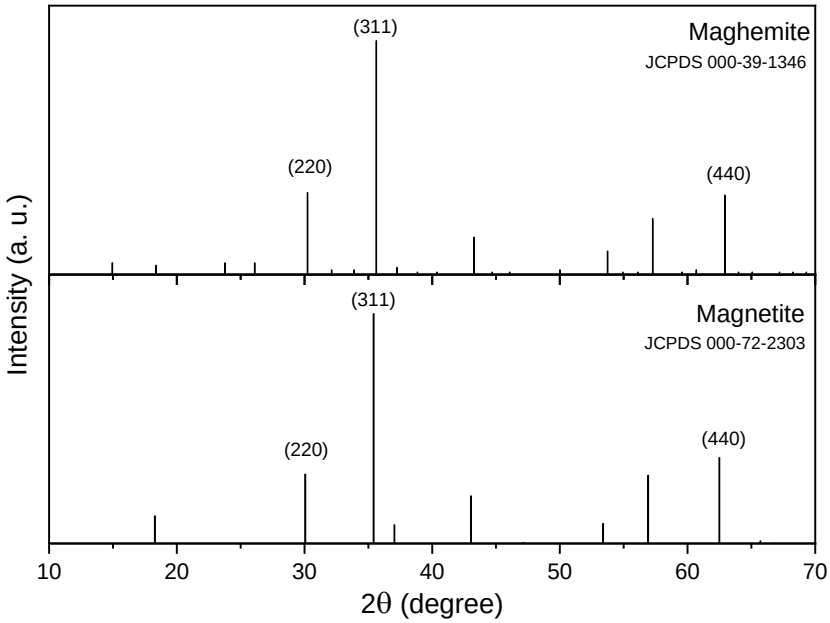

Fig. S3 XRD patterns of standart magnetite (Fe_3O_4) and maghemite (γ-Fe_2O_3) phases.

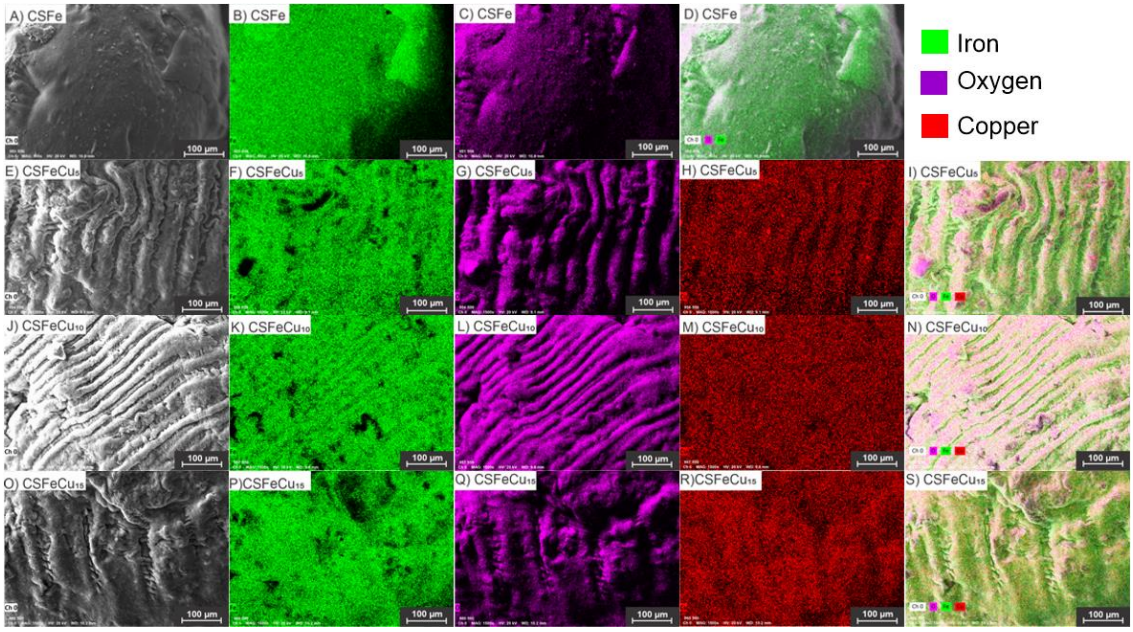

Fig. S4 Elemental mapping images of CSFe e $CSFeCu_x$.

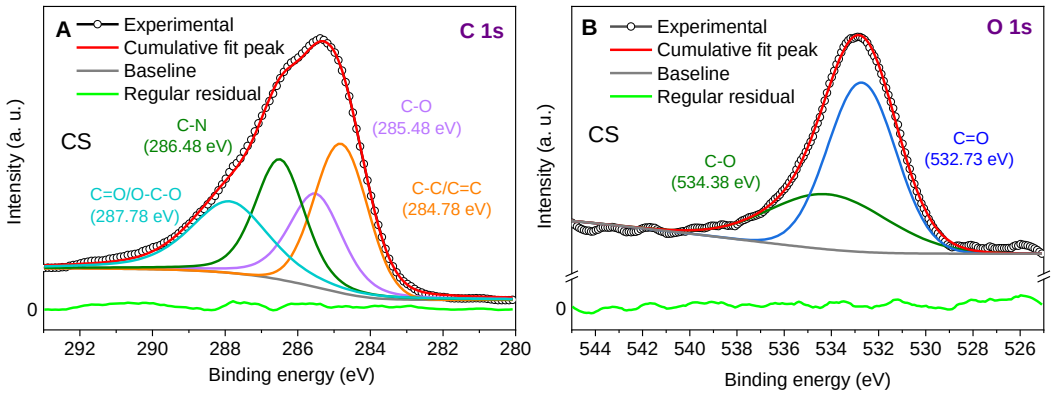

Fig. S5 XPS spectra of CS beads (a) C1s (b) O1s.

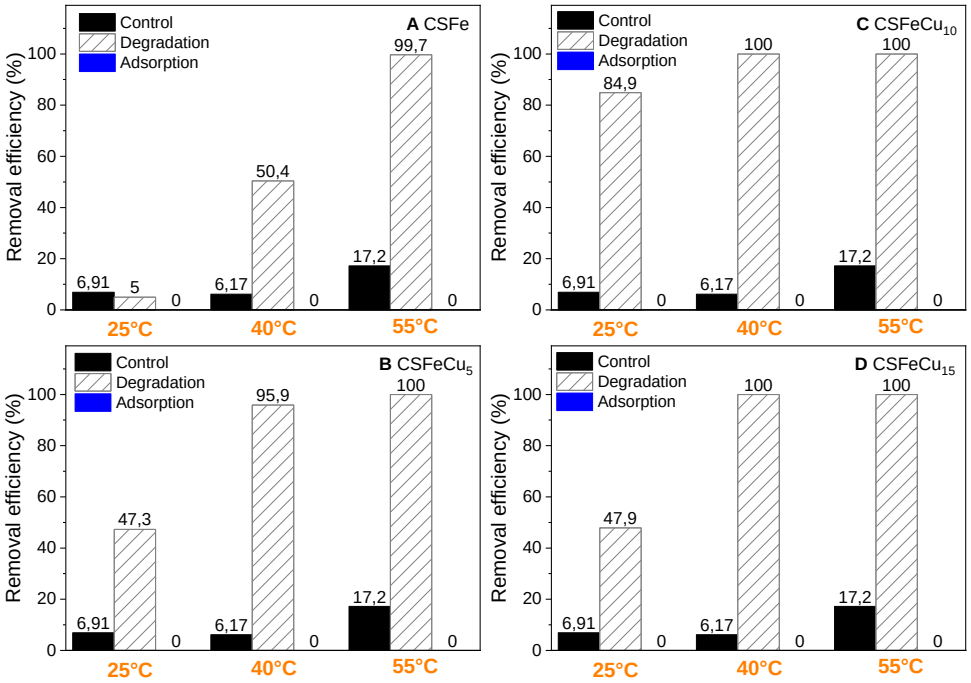

Fig. S6 Comparison between the amount of degraded and adsorbed MB, at different temperatures, by materials A) CSFe B) $CSFeCu_5$ C) $CSFeCu_{10}$ D) $CSFeCu_{15}$. 30 mg of materials; H_2O_2 (30,65 mmol L^{-1}); 29.7 ml of MB solution ± 50 mg L^{-1}; control: H_2O_2 (30,65 mmol L^{-1}) and 29.7 ml of MB solution ± 50 mg L^{-1}.

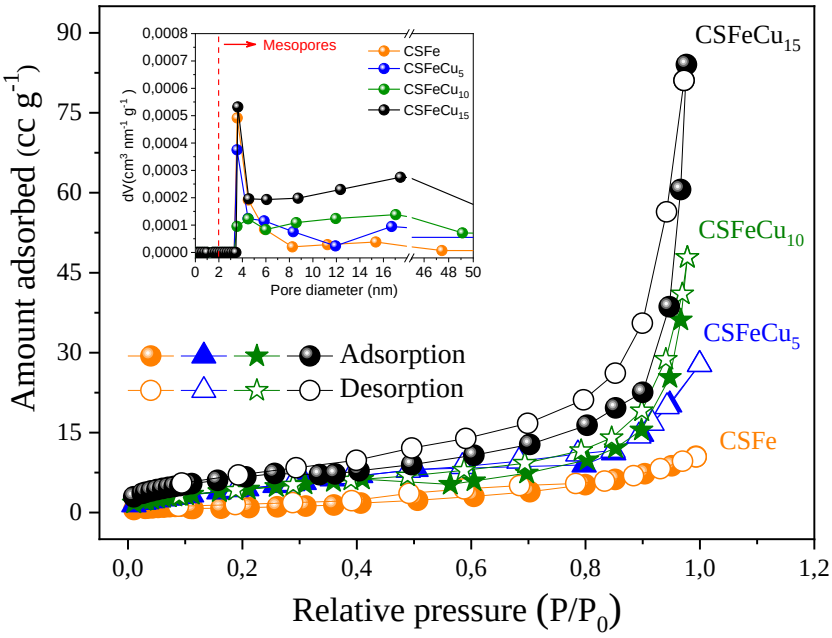

Fig. S7 Nitrogen adsorption/desorption isotherms and pore size distributions curve (inset) of CSFe and $CSFeCu_x$ beads.

Table S3 Textural properties of beads CSFe e $CSFeCu_x$.

Material	S_{BET} ($m^2\ g^{-1}$)	Total pore volume ($cm^3\ g^{-1}$)	Average pore diameter (nm)
CSFe	3,051	0,007	3,099
$CSFeCu_5$	18,61	0,014	1,682
$CSFeCu_{10}$	16,63	0,013	1,543
$CSFeCu_{15}$	23,33	0,025	1,682

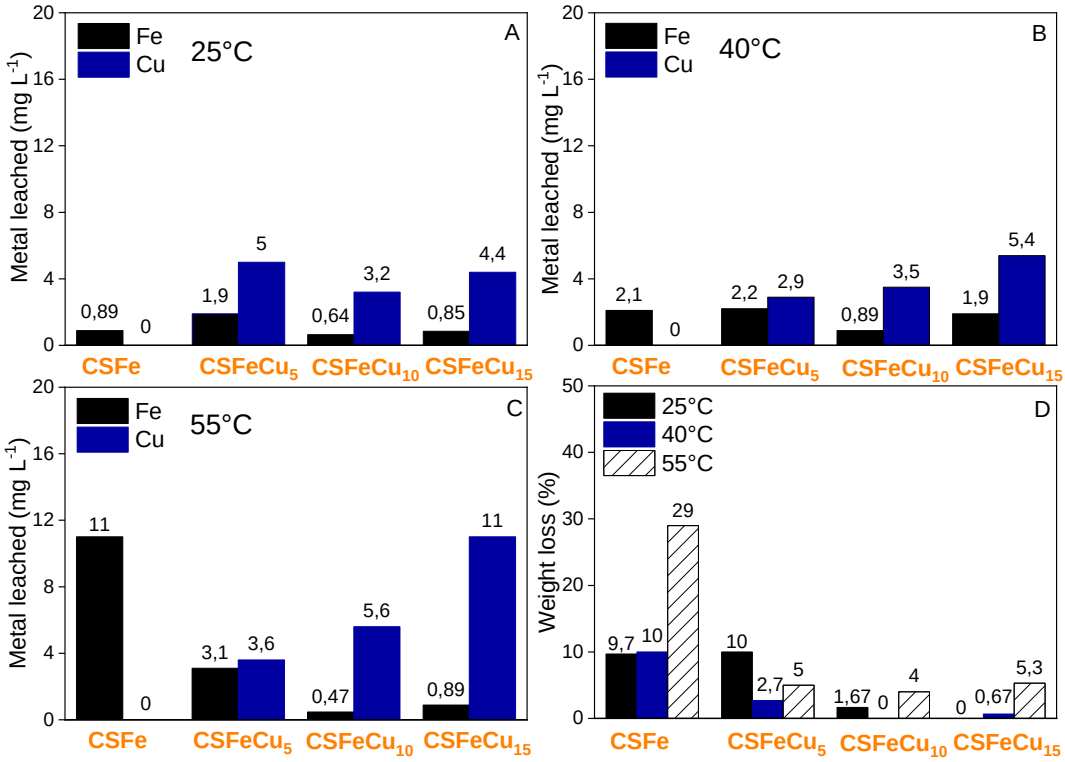

Fig. S8 Iron and copper dosage in supernatant after MB degradation at temperatures of (a) 25 (b) 40 (c) 55°C (d) Weight loss of materials after degradation of MB at temperatures of 25, 40 e 55°C.

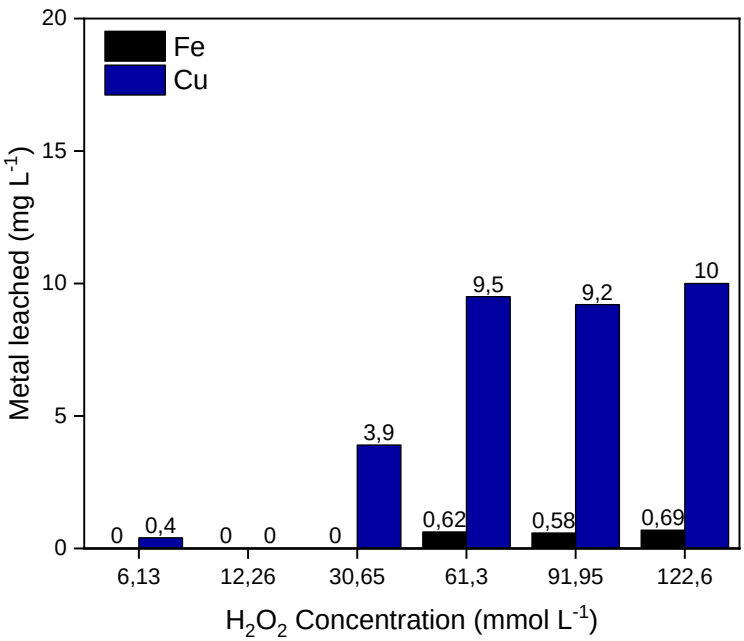

Fig. S9 Concentration of leached Fe and Cu after MB degradation by $CSFeCu_{10}$ material at different H_2O_2 concentrations.

Toxicity-hemolysis assay (Experimental methods)

Hemolytic potential of the degradation reaction products was evaluated according to the ASTM F 756 protocol. Briefly, blood samples were collected in citrated vacutainer tubes. Blood samples were centrifuged at 800xg to allow the removal of plasma without washing steps. The remaining red blood cells were suspended (PBS) in 100 mL of PBS (1.15 mM de $NaH_2PO_4.H_2O$, 4 mM de $Na_2HPO_4.H_2O$ and 0.15 M NaCl, pH 7.4) to a hematocrit equivalent of 1.5%. In 2.5 mL capped tubes it was added 1.5 mL of the PBS and 250 µL the test sample. Test samples included methylene blue controls (1/2x the standard reaction concentration, standard concentration and 2x), the same values were used for hydrogen peroxide and the degradation products. The samples were maintained in a polystyrene rack at 37°C for 2 h, and gently inverted 3 times at every 30 minutes. At the end of the incubation time, the tubes were centrifuged once again to precipitate the mass of cells. The supernatant was then collected and added 1 mL of the cyanmethemoglobin reagent read at 540 nm against a calibration curve to determine hemoglobin content. Blanks were performed to remove the colorimetric effect of the reactants. The hemolysis percentage was calculated as:

$$\text{Hemolysis } \% = \frac{(\text{SH} - \text{MH})}{(\text{TH} - \text{MH})} * 100$$

Where: SH = Sample hemoglobin content; MH = Mechanical hemoglobin, corresponds to the manipulation of the samples; TH = Total hemoglobin per tube, given by the addition of 10 µL of well-mixed pooled whole blood to 2.5 mL of cyanmethemoglobin reagent for 15 minutes.

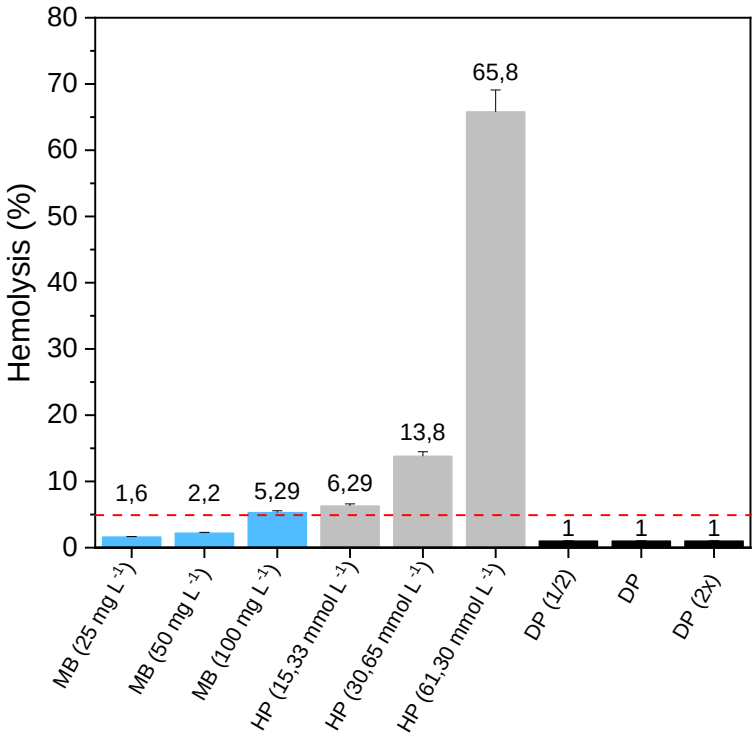

Fig. S10 Percentage of hemolysis. MB: methylene blue; HP: hydrogen peroxide; DP (1/2): half the standard concentration of the degradation reaction products; DP: standard concentration; and DP (2x): twice the standard concentration of the degradation reaction products. Data were obtained by comparison with the total amount of hemoglobin per tube; the bars represent the mean hemolysis percentage followed by the standard deviation.

References

1 P. M. B. Chagas, L. B. de Carvalho, A. A. Caetano, F. G. E. Nogueira, A.D. Corrêa, I. R. Guimarães, J. Environ. Chem. Eng., 2018, 6, 1008-1019.

2 C. Song, H. Yu, M. Zhang, Y. Yang, G. Zhang, Int. J. Biol. Macromol., 2013, 60, 347-354.

3 M. A. Hassan, A. M. Omer, E. Abbas, W. M. Baset, T. M. Tamer, Sci. Rep., 2018, 8, 11416.

4 S. Rashid, C. Shen, X. Chen, S. Li, Y. Chen, Y. Wen, J. Liu, RSC Adv., 2015, 5, 90731-90741.

5 D. Jiang, D. Huang, C. Lai, P. Xu, G. Zeng, J. Wan, L. Tang, H. Dong, B. Huang, T. Hu, Sci. Total Environ., 2018, 644, 1181-1189.